Multiscale Enrichment based on Partition of Unity for Nonperiodic Fields and Nonlinear Problems

Jacob Fish and Zheng Yuan
Departments of Civil, Mechanical and Aerospace Engineering
Rensselaer Polytechnic Institute
Troy, NY 12180, USA
fishj@rpi.edu

Abstract

We present a generalization of the Multiscale Enrichment based on Partition of Unity (MEPU) formulation originally reported in [1] to account for boundary layers, nonperiodic fields and nonlinear systems. MEPU is aimed at extending the range of applicability of the mathematical homogenization theory to nonlinear nonperiodic systems with inseparable fine and coarse scales. Performance studies for both continuum and coarse grained discrete systems are conducted to validate the formulation.

1. Introduction

Multiscale Enrichment based on the Partition of Unity or MEPU developed in [1] is a synthesis of the mathematical homogenization and the Partition of Unity (PU) methods. Its primary objective is to extend the range of applicability of the mathematical homogenization theory to problems where scale separation may not be possible. The method [1] has been applied to enriching the coarse scale continuum descriptions (PDEs) with fine scale features as well coarse grained discrete formulations with relevant atomistic data. MEPU takes advantage of the simplicity of scale bridging offered by the mathematical homogenization theory and the elegance of enforcing C^0 continuity of solution without compromising on the sparsity provided by the PU framework. It is free of some of the drawbacks inherent in each of its two constituents, namely: the discontinuity of the fine scale enrichment function arising from the mathematical homogenization theory and the complexity emanating from integrating coupling terms in the PU based methods.

MEPU falls into the category of Sparse Global Enrichment Methods (SGEM), which employ global enrichment functions, but give rise to sparse matrices as opposed to the classical global-local methods [2]. Among the noteworthy SGEMs are the s-version of the finite element method [3,4,5,6] with application to strong [7,8] and weak [9,10,11,12] discontinuities, various multigrid-like scale bridging methods [13, 14, 15, 16], the

Extended Finite Element Method (XFEM) [17,18,19], the Generalized Finite Element Method (GFEM) [20,21] and the Discontinuous Galerkin (DG) [22,23] method.

The XFEM and GFEM are based on the local [24] and global [25,26] Partition of Unity frameworks, respectively. In XFEM, the enrichment functions describe spatial features, such as asymptotic crack fields [27], local flow fields [28] as well as arbitrary discontinuities, while in GFEM, they describe special handbook function [29,30].

The primary objective of the present manuscript is to generalize the formulation of MEPU presented by the authors in [1]. The original paper [1] focused on the exposition of basic ideas including fine scale enrichment, homogenization-like integration scheme and the interface formulation between the MEPU and homogenized elements, but was limited to idealized scenarios such as: (i) linear problems, (ii) $O(1)$ enrichment functions and (iii) periodic fine scale fields. For nonlinear problems, enrichment functions have to be recomputed for optimal performance. Enrichment functions extracted from the $O(1)$ mathematical homogenization might be sufficient in the regions with moderate coarse scale gradients, but might be inadequate in the vicinity of boundary layers. Accounting for random or nonperiodic fields is not a trivial task since fine scale enrichment functions in this case are either unknown or cannot be periodically extended over the entire coarse scale problem domain.

The outline of this paper is as follows. Section 2 describes the higher order enrichment functions. Formulation for the nonperiodic fields is presented in Section 3. Generalization to nonlinear problems is given in Section 4. Verification studies follow the derivations in the corresponding sections.

2. MEPU for higher order periodic fields

2.1 Formulation

We start by stating the key result from the mathematical homogenization theory for periodic elastic heterogeneous media. Consider a three-term double-scale asymptotic expansion of the solution, $u_i = u_i^0(\boldsymbol{x}) + \zeta u_i^1(\boldsymbol{x},\boldsymbol{y}) + \zeta^2 u_i^2(\boldsymbol{x},\boldsymbol{y})$, where $\boldsymbol{x}$ and $\boldsymbol{y} = \boldsymbol{x}/\zeta$ are the coarse and fine scale position vectors, respectively; $0 < \zeta = l/L \ll 1$, and l, L denote the characteristic size of the fine and coarse scale, respectively. In reference [1], only the first order term decomposed as

$$\begin{aligned} u_i^1(\boldsymbol{x},\boldsymbol{y}) &= \chi_{ikl}(\boldsymbol{y})\varepsilon_{kl}^0(\boldsymbol{x}) \\ \varepsilon_{ij}^0 &\equiv u_{(i,x_j)}^0 = (u_{i,x_j}^0 + u_{j,x_i}^0)/2 \end{aligned} \tag{1}$$

was considered for the enrichment. In (1) $\chi_{ikl}(\boldsymbol{y})$ is the first order influence function (symmetric with respect to *kl* indices). The approximation of solution field was constructed by replacing ε_{kl}^0 and $\zeta\chi_{ikl}(\boldsymbol{y})$ in Eq. (1) with an independent set of degrees-

of-freedom $a_{kl\alpha}$ and the influence functions defined over the local supports $\chi_{ikl}(\boldsymbol{x})N_\alpha(\boldsymbol{x})$, respectively.

In the present manuscript, we consider the second order term of the fine scale solution. Following [31], the decomposition of the second order term is given as

$$u_i^2(\boldsymbol{x},\boldsymbol{y}) = \eta_{ijmn}(\boldsymbol{y})\varepsilon^0_{mn,x_j}(\boldsymbol{x}) \tag{2}$$

where $\eta_{ijmn}(\boldsymbol{y})$ is the second order influence function to be used as the second order enrichment in MEPU. Using a similar procedure as for the first term enrichment, we constructs the second order enrichment by replacing $\varepsilon^0_{mn,j}$ and $\zeta^2\eta_{ijmn}(\boldsymbol{y})$ in Eq. (2) with a set of independent degrees-of-freedom $b_{jmn\alpha}$ and the second order influence functions defined over the local supports $\eta_{ijmn}(\boldsymbol{x})N_\alpha(\boldsymbol{x})$, respectively.

It is convenient to replace the pair of subscripts kl in χ_{ikl} and $a_{kl\alpha}$ denoting the first order enrichment modes by a single upper case Roman subscript, *A*. Likewise, we replace the subscripts jmn in η_{ijmn} and $b_{jmn\alpha}$ denoting the second order enrichment modes by another single upper case Roman subscript, *B*. The resulting enriched solution approximation states

$$u_i = \bar{N}_\beta(\boldsymbol{x})d_{i\beta} + N_\alpha(\boldsymbol{x})\left[\chi_{iA}(\boldsymbol{x})a_{A\alpha} + \eta_{iB}(\boldsymbol{x})b_{B\alpha}\right] \tag{3}$$

where summation convention is employed for the repeated indices; Greek subscripts denote finite element nodes. Note that the shape functions used for the coarse scale discretization, $\bar{N}_\beta(\boldsymbol{x})$, might be different from those used in the partition of unity decomposition $N_\alpha(\boldsymbol{x})$. Numerical experiments in Section 2.2 suggest that for nearly optimal performance with lower order elements $\bar{N}_\beta(\boldsymbol{x})$ should be quadratic while $N_\alpha(\boldsymbol{x})$ linear. It is instructive to note that while in the mathematical homogenization theory χ_{iA} and η_{iB} are functions of the fine scale coordinate, *y*, in MEPU, χ_{iA} and η_{iB} serve to forming the enriched shape functions expressed in term of a single physical coordinate, *x*.

With the second order enrichment in place, MEPU is equipped with the deformation modes capable of capturing linear variation of coarse scale strain gradients over the unit cell domain. Such an enrichment is necessary in the high gradients region, such as in the vicinity of cracks or cutouts where the characteristic size of the unit cell is comparable to the coarse scale features. Nevertheless, the second order enrichment involves additional degrees-of-freedom, and therefore should be used in the critical regions only.

For linear problems, the influence functions $\chi_{ikl}(\boldsymbol{y})$ and $\eta_{ijmn}(\boldsymbol{y})$ in Eq. (3) can be precomputed by solving a unit cell problem (s). The continuum version of the unit cell problem for $\chi_{ikl}(\boldsymbol{y})$ is given by

$$\begin{aligned}
&\left[L_{ijkl}\left(\chi_{mn(k,y_l)}+I_{klmn}\right)\right]_{,y_j}=0 \;\; on \;\; \Theta \\
&\chi_{imn}(\boldsymbol{y})=\chi_{imn}(\boldsymbol{y}+\hat{\boldsymbol{y}}) \quad on \quad \partial\Theta \\
&\chi_{imn}(\boldsymbol{y})=0 \;\; on \quad \partial\Theta^{vert}
\end{aligned} \tag{4}$$

where $\partial\Theta$ is the unit cell boundary and $\partial\Theta^{vert}$ are the vertices of the unit cell; L_{ijkl} - the linear elasticity constitutive tensor; $I_{klmn}=\left(\delta_{mk}\delta_{nl}+\delta_{nk}\delta_{ml}\right)/2$; $\hat{\boldsymbol{y}}$ is the basic period of the unit cell; Eq. (4)c is often replaced by the normalization condition $\int_{\Theta}\chi_{ikl}d\Theta=0$. For the formulation of the discrete unit cell problem we refer to [32].

Once the solution of Eq. (4) is obtained, $\eta_{ijmn}(\boldsymbol{y})$ can be determined through the following unit cell problem

$$\begin{aligned}
&\left[L_{iskl}\left(\chi_{mnk}\delta_{jl}+\eta_{jmn(k,y_l)}\right)\right]_{,y_s}+L_{ijkl}\left(\chi_{mn(k,y_l)}+\delta_{mk}\delta_{nl}\right)-\bar{L}_{ijmn}=0 \quad on \quad \Theta \\
&\eta_{jmnk}(\boldsymbol{y})=\eta_{jmnk}(\boldsymbol{y}+\hat{\boldsymbol{y}}) \quad on \quad \partial\Theta \\
&\eta_{jmnk}(\boldsymbol{y})=0 \;\; on \quad \partial\Theta^{vert}
\end{aligned} \tag{5}$$

where $\bar{L}_{ijmn}$ is the homogenized constitutive tensor given as

$$\bar{L}_{ijmn}=\frac{1}{|\Theta|}\int_{\Theta}L_{ijkl}\left(\chi_{mn(k,y_l)}+I_{klmn}\right)d\Theta \tag{6}$$

The two unit cell problems are typically solved using finite element method. The stiffness matrix for the higher order unit cell problem (5) is identical to that of the $O(1)$ unit cell problem, whereas the right hand side vector depends on the solution of the $O(1)$ problem. For the implementation details we refer to [31].

The discrete system of coarse scale equations is obtained using standard Galerkin method (see for instance [19,20]) and the Homogenization-Like Integration (HLI) scheme developed in [1].

Remark 1: The main difference between the mathematical homogenization and MEPU is that the influence functions χ_{iA} and η_{iB} in the mathematical homogenization are multiplied by known macroscopic fields, $\boldsymbol{\varepsilon}^0(\boldsymbol{x})$ and $\nabla\boldsymbol{\varepsilon}^0(\boldsymbol{x})$, respectively. In MEPU, however, these influence functions are multiplied by unknown coefficients, which are found from the weak form on a subspace. Certainly, the resulting method is more expensive than the homogenization theory because of the introduction of new variables and yet, numerical experiments conducted in [1] and in the present manuscript suggest significant gains in accuracy.

2.2 Verification

In this section, the second order MEPU formulation is verified for a two-dimensional linear elastic fracture problem. The geometry and boundary conditions of the model problem are shown in Figure 1a. The uniform displacement boundary condition is applied along the top and bottom edges of the plate. Due to symmetry, only the upper half of the plate is analyzed.

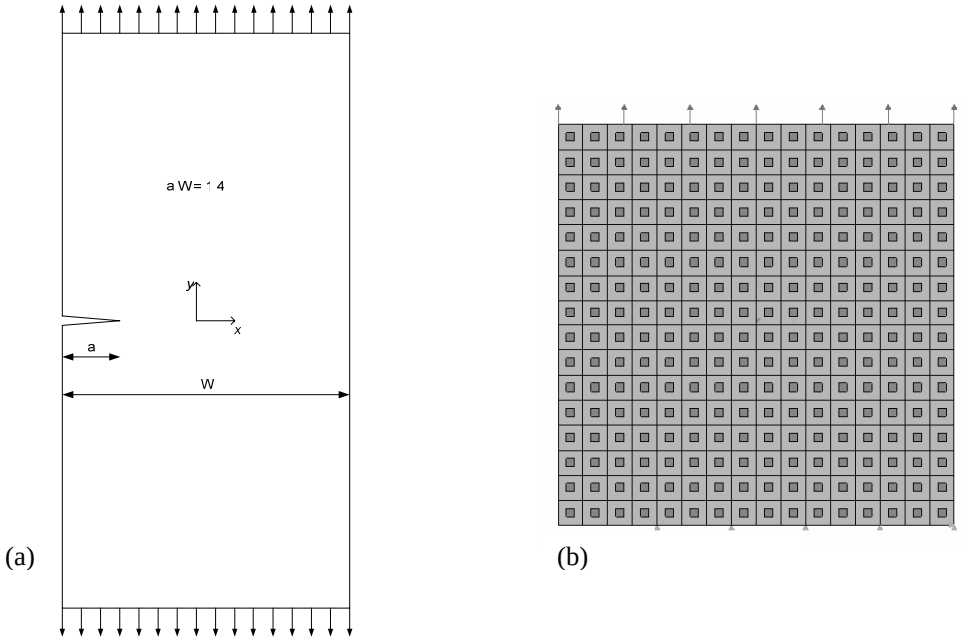

Figure 1: Configuration for the two-dimensional linear elastc fracture problem:
(a) problem domain and loading; (b) material distribution

The heterogeneous properties are represented by a unit cell with a square inclusion. One half of the problem domain consists of 16x16 unit cells as shown in Figure 1b. The phase properties of the fine scale constituents are listed in Table I.

Table I: Material properties for the two-dimensional unit cell

	Young's Modulus (GPa)	Poisson's ratio
Inclusion Material	60	0.2
Matrix Material	2	0.2

The reference solution is obtained using a fine mesh with each unit cell discretized by 6x6 quadratic elements, totaling 9216 elements. For comparison, three methods are investigated: (i) mathematical homogenization (HOMO) on the entire problem domain, discretized with 16x16 quadratic finite elements possessing homogenized properties; (ii) as in (i) but replacing 2x4 HOMO elements around the crack tip by the $O(1)$ MEPU elements; (iii) as in (ii), but replacing the closest two $O(1)$ MEPU elements around the crack tip by the second order MEPU elements (denoted as $O(\varepsilon)$ MEPU). The polynomial order of the coarse scale fields in the two MEPU versions is quadratic. All the meshes are shown in Figure 2.

The results of the total strain energy and the stress intensity factor are summarized in Table II. The stress intensity factors were evaluated using the virtual crack closure integral method [33]. It can be seen that by adding higher order enrichment functions in just two elements in the critical region the quality of the solution can be significantly improved.

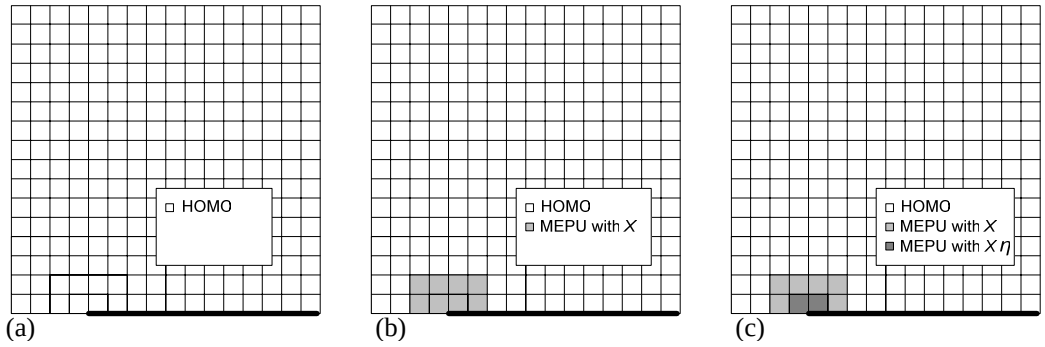

Figure 2: Mixed mesh for the two-dimensional linear elastic fracture problem:

(a) the HOMO mesh; (b) the HOMO $O(1)$ MEPUmesh; (c) the HOMO $O(1)$ & $O(\varepsilon)$ MEPU mesh

Table II: Numerial results for the two-dimensional linear elastic fracture problem

Methods	Total Strain Energy		Stress Intensity Factor	
	E	Error (%)	K	Error (%)
HOMO	1.1015E+07	2.26	1.2795E+06	4.53
$O(1)$ MEPU	1.0980E+07	1.93	1.2595E+06	2.89
$O(\varepsilon)$ MEPU	1.0840E+07	0.63	1.2144E+06	0.79
REF	1.0772E+07	-	1.2241E+06	-

3. Generalization to nonperiodic and random fields

3.1 Formulation

The formulation of MEPU presented in Section 2 is limited to periodic fields. Periodicity is required to extend the local enrichment functions χ_{ijk}, η_{ijkl} over the entire (or portion of) coarse scale problem domain. In general, however, not only that the fields may not be periodic, their microstructure may not be known. At best, one can only sample (or scan) for the microstructure characteristics at some discrete points as shown in Figure 3. Thus the enrichment functions and therefore the element shape functions may not be known over the entire problem domain. From the formulation point of view material data are required at the coarse scale elements Gauss points only. From the practical point of view, the experimental sampling data and the finite element mesh data have to be completely independent. Thus in practice, experimental measurements are carried out independently at some discrete points and then material data is assigned to the corresponding coarse scale elements.

With this in mind, let $\hat{\chi}_{iA} = \cup \chi^I_{iA}$ denote the union of influence functions computed over the unit cell domains Θ^I positioned at the coarse scale elements Gauss points. The solution approximation defined over the unit cell domains is given as

$$u_i = N_\beta(\boldsymbol{x}) d_{i\beta} + \hat{\chi}_{iA}(\boldsymbol{x}) N_\alpha(\boldsymbol{x}) a_{A\alpha} \tag{7}$$

where for simplicity of illustration the $O(1)$ MEPU approximation is employed.

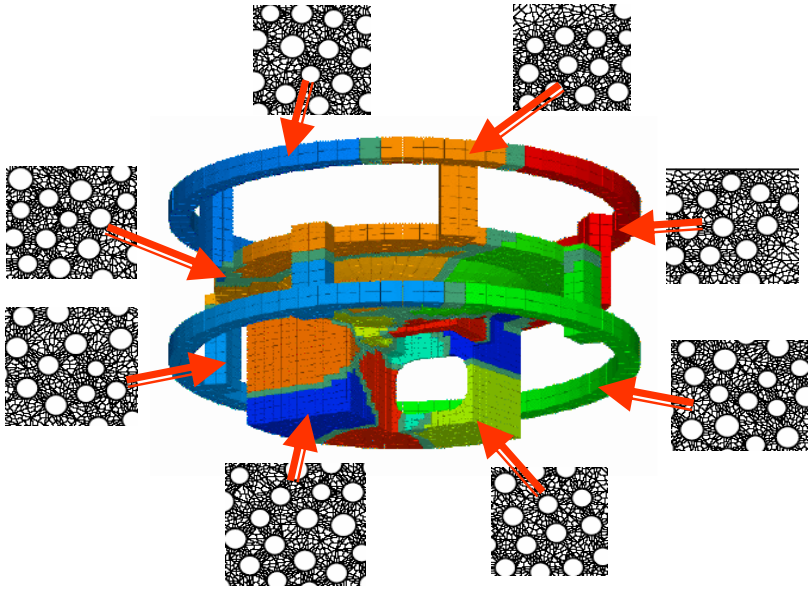

Figure 3: Assigning different microstructure to various global subdomains

The discrete system of equations is obtained using the standard Galerkin method. Various integrals are evaluated using Homogenization-Like Integration (HLI) scheme developed and analyzed in [1] with only exception that the integrand at the coarse scale element Gauss points is a function of the influence function computed from the unit cell solution positioned at that point. Thus the integration scheme can be expressed as

$$I = \int_{\square} J f d\square = \sum_{I=1}^{ngauss} W_I J_I f_I\left(\chi^I\right) = \sum_{I=1}^{ngauss} W_I J_I \frac{1}{|\Theta|} \int_{\Theta_I} f\left(\chi^I\right) d\Theta \tag{8}$$

where $\square$ is the biunit parent domain, W the weight function, J the Jacobian, and *ngauss* the number of quadrature points.

The HLI scheme schematically depicted in Figure 4, positions the unit cell at the center of each coarse scale Gauss points. The value of the integrand at the coarse scale Gauss point is replaced by the integral over the unit cell domain normalized by the volume of the unit cell.

Remark 1: When solving Eq. (4) for different unit cells, application of periodic boundary condition may not be appropriate. Moreover, for nonperiodic fields the unit

cells could be of arbitrary shape subjected to Dirichlet boundary conditions. An alternative strategy consists of defining somewhat larger domain than that of the unit cell, applying appropriate Dirichlet boundary conditions, and then computing the influence functions from the data extracted from the original unit cell domain [34].

Remark 2: For highly randomly microstructure, Homogenization-Like Integration (HLI) scheme may not be sufficiently accurate; therefore integration over the entire coarse element domain might be needed instead.

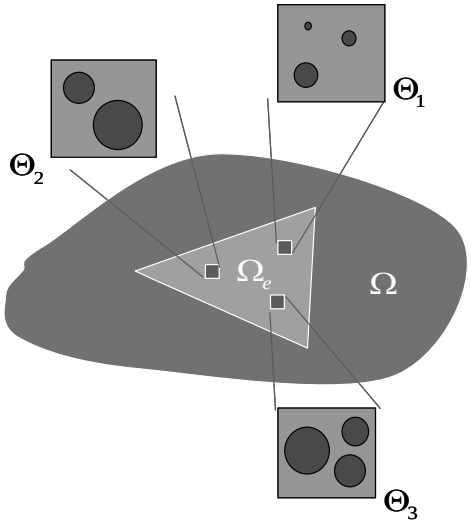

Figure 4: Modified HLI scheme for nonperiodic fields

3.2 Verification

In this section MEPU formulation for nonperiodic fields is studied in the context of enriching continuum and discrete coarse-grained descriptions. We first consider a two-dimensional continuum problem as shown in Figure 5. The problem domain consists of circular inclusions of various diameter sizes randomly distributed in a matrix material. A uniform displacement boundary condition in the vertical direction is applied along the top edge. Symmetric essential boundary conditions are applied along the left and the bottom edges of the model.

For the reference solution, the domain was discretized with 129,260 triangular elements, with a typical element size smaller than of the smallest inclusion. For the $O(1)$ MEPU formulation, the domain was modeled with eight coarse scale triangular elements. For each coarse scale element, three different unit cell problems positioned at the element Gauss points have been analyzed to obtain the influence functions. Each unit cell problem was discretized with approximately 500 elements. Figure 4 depicts the coarse scale mesh consisting of 8 triangles as well as 24 unit cells.

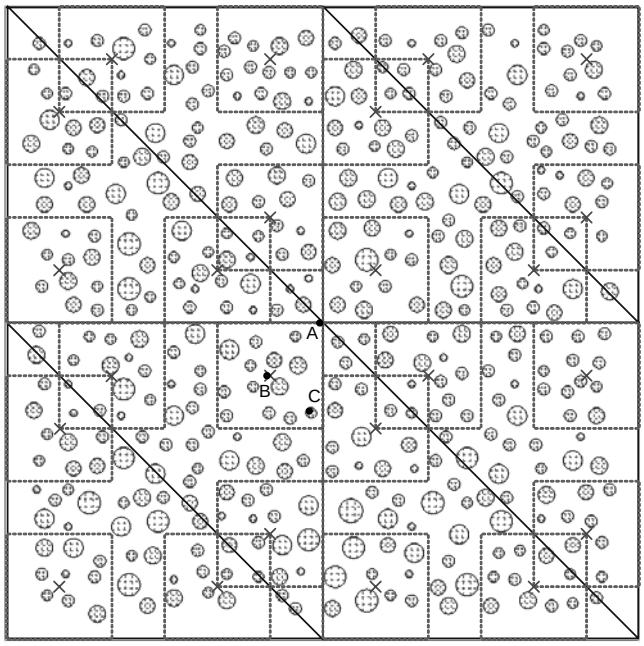

Figure 5: nonperiodic continuum problem

The results of the total strain energy and the strain component ε_{22} at three arbitrary selected points shown in Figure 5 are summarized in Table III. We compare the MEPU results with the homogenization method (HOMO) and the reference solution. For the homogenization methods, we employ the same nonperiodic influence functions used in MEPU to compute the homogenized constitutive tensor.

Table III: Numerial results for the two-dimensional linear elastic fracture problem

Methods	Total Strain Energy Error (%)	Strain ε_{22}		
		Error (%) - A	Error (%) - B	Error (%) - C
HOMO	2.65	9.69	8.57	5.97
MEPU	0.55	3.81	3.32	3.48

For the second example, we consider a coarse grained discrete system: a linear homopolymer model with 32 chains (each chain is made up of 16 identical repeating monomers) as shown in Figure 6.

For simplicity, only two types of the interaction potentials are considered: strong bonding potential between the neighboring units belonging to the same chain and the weak interaction between the remaining units. The quadratic approximation of the Lennard-Jones potential

$$E_a(r) = -\varepsilon_1 + \frac{1}{2}a\left(r - r_0^1\right)^2,\ E_b(r) = -\varepsilon_2 + \frac{1}{2}b\left(r - r_0^2\right)^2 \tag{9}$$

has been employed, where $r_0^k\ (k=1,2)$ are the interatomic distances at the equilibrium; a and b are constants defined by: $a=\frac{36\sqrt[3]{4}\varepsilon_1}{\sigma_1^2}$ and $b=\frac{36\sqrt[3]{4}\varepsilon_2}{\sigma_2^2}$, where $\sigma_1=3.405\times10^{-10}$, $\varepsilon_1=2.0288\times10^{-18}$; $\sigma_2=3.405\times10^{-10}$, $\varepsilon_2=2.0288\times10^{-21}$. The cut off distance for the weak interactions is defined as 1.5 lengths between the neighboring units in a chain. The polymer model consists of total 480 and 1239 strong and weak bonds, respectively.

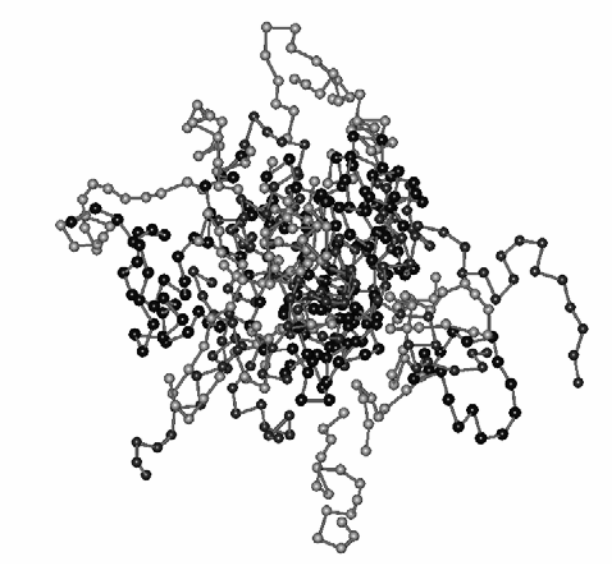

Figure 6: the initial configuration of the polymer model

The model is subjected to a constant coarse scale strain field in x-direction. The displacement results for each unit are obtained using molecular mechanics (the reference solution), MEPU and quasi-continuum (QC) method based on the Born rule. Table IV summarizes the total number of the degrees-of-freedom used in each method and the relative error in L_2 norm and maximum norms of displacements.

Table IV: Numerial results for the polymer problem

Methods		REF	MEPU	QC
The Number of DOF		654	72	24
Displacement error in:	L_2 Norm	-	2.18%	8.94%
	Maximum Norm	-	8.44%	26.55%

4. Extension to nonlinear problems

4.1 Formulation

In this section MEPU is generalized to nonlinear problems. For simplicity, attention is restricted to material nonlinearity and rate-independent plasticity model. As a prelude, we summarize the basic equations of nonlinear mathematical homogenization, which serve the foundation for the nonlinear variant of MEPU. Derivation details can be found in Appendix A.

We start with the governing equations defined on the finest scale of interest

$$\begin{aligned}
&\sigma^{\zeta}_{ij,x_j} + b_i = 0 \quad on \quad \Omega \\
&\dot{\sigma}^{\zeta}_{ij} = L^{\zeta}_{ijkl}\left(\underset{\sim}{\sigma}\right)\dot{\varepsilon}^{\zeta}_{kl} \\
&\dot{\varepsilon}^{\zeta}_{kl} \equiv \dot{u}^{\zeta}_{(k,x_l)} = \left(\dot{u}^{\zeta}_{k,x_l} + \dot{u}^{\zeta}_{l,x_k}\right)/2 \\
&u_i = g_i \quad on \quad \Gamma_g \\
&\sigma_{ij} n_j = t_i \quad on \quad \Gamma_t
\end{aligned} \tag{10}$$

where L^{ζ}_{ijkl} is the instantaneous elasto-plastic constitutive tensor, and $\dot{\square} \equiv \frac{d}{dt}\square$.

For the $O(1)$ homogenization theory a two-term asymptotic expansions of the velocity field is employed

$$\dot{u}^{\zeta}_i\left(\boldsymbol{x}\right) = \dot{u}^0_i\left(\boldsymbol{x}\right) + \zeta \dot{u}^1_i\left(\boldsymbol{x},\boldsymbol{y}\right) + O\left(\zeta^2\right) \tag{11}$$

where the first term is assumed to be independent of the fine scale details. Separation of variables for the second term in the velocity field yields

$$\dot{u}^1_k = \chi_{mnk}\left(\boldsymbol{y}\right)\dot{\varepsilon}^0_{mnx}\left(\boldsymbol{x}\right) \tag{12}$$

where symmetric coarse scale velocity gradient $\dot{\varepsilon}^0_{mnx}\left(\boldsymbol{x}\right)$ is defined as

$$\dot{\varepsilon}^0_{mnx} \equiv \dot{u}^0_{(m,x_n)} = \frac{1}{2}\left(\frac{\partial \dot{u}^0_m}{\partial x_n} + \frac{\partial \dot{u}^0_n}{\partial x_m}\right)$$

The $O\left(\zeta^{-1}\right)$ rate equilibrium equation gives a unit cell (fine scale) problem

$$\begin{aligned}
&\left[L_{ijkl}\left(I_{klmn} + \phi_{mnkl}\right)\right]_{,y_j} = 0 \\
&\phi_{mnkl} \equiv \chi_{mn(k,y_l)} = \left(\chi_{mnl,y_k} + \chi_{mnk,y_l}\right)/2
\end{aligned} \tag{13}$$

where material properties in the unit cell $L_{ijkl}\left(\boldsymbol{y},t\right)$ and therefore $\chi_{klm}\left(\boldsymbol{y},t\right)$ are history-dependent. The coarse scale properties are given as $\bar{L}_{ijmn} = \frac{1}{|\Theta|}\int_{\Theta} L_{ijkl}\left(I_{klmn} + \phi_{mnkl}\right)d\Theta$.

The resulting $O(1)$ coarse scale equilibrium equation is given as

$$\left[\bar{\sigma}_{ij}\right]_{,x_j} + \bar{b}_i = 0 \tag{14}$$

Since the instantaneous constitutive tensor is nonlinear function of stresses, it is necessary to integrate the fine scale constitutive equations along the prescribed loading path in order to obtain the current stress state. For simplicity, we adopt a simple predictor-corrector update algorithm. For the implicit algorithm and for extension to large deformation plasticity we refer to [35]. The basic predictor-corrector mathematical homogenization algorithm is outlined below:

1. *Coarse scale solution phase*

   1a. Using Newton's method for the coarse scale problem, find the coarse scale displacement increment $\Delta u^0_{k\alpha}$

   1b. Compute the coarse scale strain increment

$$\begin{aligned} \Delta\varepsilon^0_{mnx} &= B_{mnk\alpha}\Delta u^0_{k\alpha} \\ B_{mnk\alpha} &= \left(N_{\alpha,m}\delta_{nk} + N_{\alpha,n}\delta_{mk}\right)/2 \end{aligned} \tag{15}$$

2. *Predictor phase* (for each Gauss point in the unit cell)

   2a. Predict the fine scale strain increment using the influence function computed from the previous time step

$$\Delta\varepsilon^0_{kl} = \left(I_{klmn} + \phi^{(n)}_{mnkl}\right)\Delta\varepsilon^0_{mnx} \tag{16}$$

   where the superscript $(\bullet)$ denotes the time step.

   2b. Use the standard stress integration procedure to update the fine scale stress $\sigma^{(n+1)}_{ij}$ (see [36] for variety of methods).

   2c. Recompute the fine scale instantaneous properties $L^{(n+1)}_{ijkl}$

3. *Corrector phase* (for each Gauss point in the coarse scale elements)

   3a. Given the updated values of the fine scale instantaneous properties $L^{(n+1)}_{ijkl}$ solve for the unit cell problem to obtain $\phi^{(n+1)}_{mnkl}$

$$\left[L^{(n+1)}_{ijkl}\left(I_{klmn} + \phi^{(n+1)}_{mnkl}\right)\right]_{,y_j} = 0 \tag{17}$$

   3b. Correct the fine scale strain increment using the average value of the influence function obtained at the previous and the current time steps (for each Gauss point in the unit cell)

$$\Delta\varepsilon^0_{kl} = \left[I_{klmn} + \frac{1}{2}\left(\phi^{(n)}_{mnkl} + \phi^{(n+1)}_{mnkl}\right)\right]\Delta\varepsilon^0_{mnx} \tag{18}$$

   3c. Update the fine scale stress field $\sigma^{(n+1)}_{ij}$ using one of the standard stress update procedures.

4. *Coarse scale solution update phase*

4a. Using the corrected values of $\phi_{ijkl}^{(n+1)}$ and $L_{ijkl}^{(n+1)}$, update the homogenized instantaneous properties

$$\bar{L}_{ijkl}^{(n+1)} = \frac{1}{|\Theta|}\int_{\Theta} L_{ijkl}^{(n+1)}\left(I_{klmn} + \phi_{mnkl}^{(n+1)}\right)d\Theta \tag{19}$$

4b. Update for the overall stress using the corrected values of $\sigma_{ij}^{(n+1)}$

$$\bar{\sigma}_{ij}^{(n+1)} = \frac{1}{|\Theta|}\int_{\Theta} \sigma_{ij}^{(n+1)} d\Theta \tag{20}$$

We now turn to the MEPU predictor-corrector algorithm, which is closely related to the aforementioned nonlinear homogenization procedure. The main difference between the two is that the fine and coarse scales in MEPU are simultaneously evolved. The computational cost of the fine scale computations is similar, but the solution phase in MEPU is computationally more involved since the system of equation to be solved consists of coarse scale and enrichment degrees-of-freedom. The MEPU predictor-corrector algorithm is summarized below:

1. *Solution phase*

   Using Newton's method find the coarse and fine scale displacement increments $\Delta d_{m\alpha}$, $\Delta a_{pq\alpha}$, respectively.

2. *Predictor phase* (for each Gauss point in the unit cell)

   2a. Predict the fine scale strain increment using the influence functions computed from the previous time step

$$\begin{aligned} \Delta\varepsilon_{kl}^{0} &= \underbrace{B_{klm\alpha}}_{\boldsymbol{B}^1}\Delta d_{m\alpha} + \underbrace{\left(\phi_{pqkl}^{(n)} N_{\alpha} + B_{klm\alpha}\chi_{pqm}^{(n)}\right)}_{\boldsymbol{B}^2}\Delta a_{pq\alpha} \\ \phi_{pqkl}^{(n)} &= \chi_{pq(k,y_l)}^{(n)} \end{aligned} \tag{21}$$

   2b. Use one of the standard stress integration procedures compute the fine scale stress $\sigma_{ij}^{(n+1)}$

   2c. Recompute the fine scale instantaneous properties $L_{ijkl}^{(n+1)}$

3. *Corrector phase* (for each Gauss point in the coarse scale elements)

   3a. Given the updated values of the fine scale instantaneous properties $L_{ijkl}^{(n+1)}$ solve for the unit cell problem for $\phi_{mnkl}^{(n+1)}$ and $\chi_{pqm}^{(n+1)}$ following Eq. (17).

   3b. Update the $\mathbf{B}^{(n+1)} = \left[\boldsymbol{B}^1 \quad \boldsymbol{B}^2\right]$ using Eq. (21).

   3c. Correct the fine scale strain $\Delta\varepsilon_{kl}^{0}$

$$\Delta\varepsilon_{kl}^{0} = B_{klm\alpha}\Delta d_{m\alpha} + \left[\frac{1}{2}\left(\phi_{pqkl}^{(n)} + \phi_{pqkl}^{(n+1)}\right)N_{\alpha} + \frac{1}{2}\left(\chi_{pqm}^{(n)} + \chi_{pqm}^{(n+1)}\right)B_{klm\alpha}\right]\Delta a_{pq\alpha} \tag{22}$$

3d. Update the fine scale stress field $\boldsymbol{\sigma}^{(n+1)}$ using one of the standard stress update procedures.

4. *Homogenization-like Integration(HLI) phase*

Using the updated values of $\boldsymbol{\sigma}^{(n+1)}$, $\mathbf{B}^{(n+1)}$ and $\mathbf{L}^{(n+1)}$ update the internal force vector and the tangent stiffness matrix using HLI scheme

$$\begin{aligned} \mathbf{f}^{int} &= \mathop{\boldsymbol{A}}_{e=1}^{numel} \sum_{I=1}^{ngauss} W_I J_I \frac{1}{|\Theta|} \int_{\Theta_I} \left(\mathbf{B}^{(n+1)}\right)^T \boldsymbol{\sigma}^{(n+1)} d\Theta \\ \mathbf{K} &= \mathop{\boldsymbol{A}}_{e=1}^{numel} \sum_{I=1}^{ngauss} W_I J_I \frac{1}{|\Theta|} \int_{\Theta_I} \left(\mathbf{B}^{(n+1)}\right)^T \mathbf{L}^{(n+1)} \mathbf{B}^{(n+1)} d\Theta \end{aligned} \tag{23}$$

where $\boldsymbol{A}$ is the assembly operator and *numel* is the number of elements.

4.2 Verification

In this section we consider a three-dimensional composite plate with a crack as shown in Figure 7a. Rate-independent plasticity with isotropic hardening is assumed for the matrix phase, whereas fibers are assumed to behave elastically. The phase properties are summarized in Table V.

Table V: Material properties for the three-dimensional unit cell

Materials	Young's Modulus	Poisson's ratio	Initial yield stress	Hardening modulus	Volume fraction
Titanium Matrix	68.9 GPa	0.33	24 MPa	14 GPa	0.73
SiC Fiber	379.2 GPa	0.21	-	-	0.27

For the reference solution, the composite plate was discretized with 140,400 finite elements. For the MEPU and the mathematical homogenization method (HOMO), only 400 elements were considered. In both MEPU and HOMO formulations, the region which is far away from the crack tip (shaded region in Figure 7b) was modeled with linear homogenized elements. Details of the interface formulation can be found in [1].

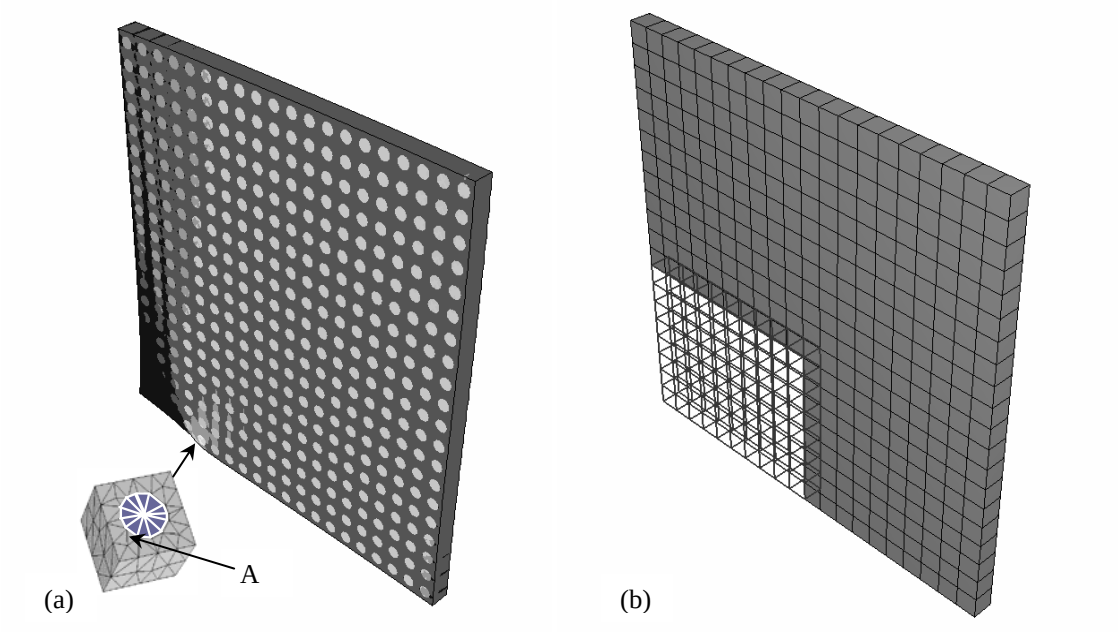

Figure 7: Configuration for the three-dimensional fracture problem:
(a) the configuration of the model and the unit cell; (b) MEPU (HOMO) mesh

The problem has been solved incrementally with ten load increments. The MEPU and HOMO formulations were compared to the reference solution in Figures 8 to 10. Figure 8 depicts the relative errors in the external work. Figure 9 gives the relative error in the local stress component σ_{22} in the loading direction at an arbitrary selected point in the vicinity of the crack tip (point A shown in Figure 7a). Figure 10 shows the relative error in the overall stress component $\bar{\sigma}_{22}$ in the nearest unit cell at the crack tip. It can be seen that MEPU formulation improves the accuracy of the solution compared to the mathematical homogenization approach, but obviously at the expense of additional degrees-of freedom, yet at a substantially lower computational cost than of the reference solution.

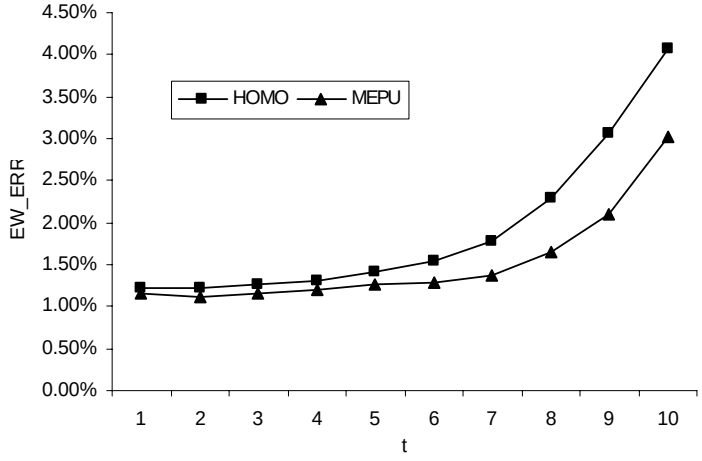

Figure 8: The relative error in the external work vs. load increment

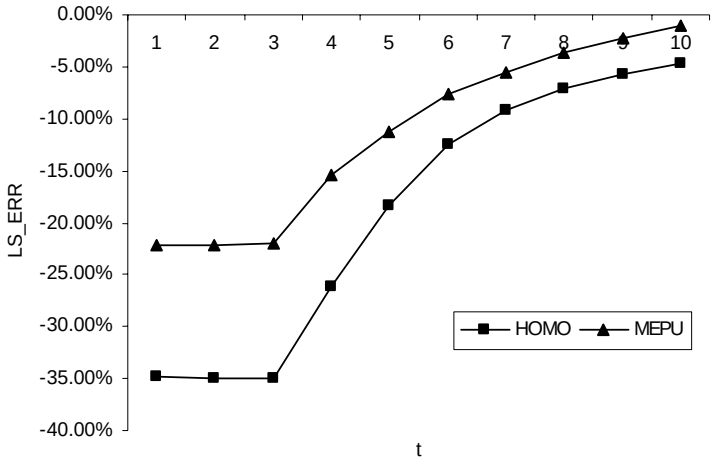

Figure 9: The relative error in the local stress σ_{22} vs. load increment

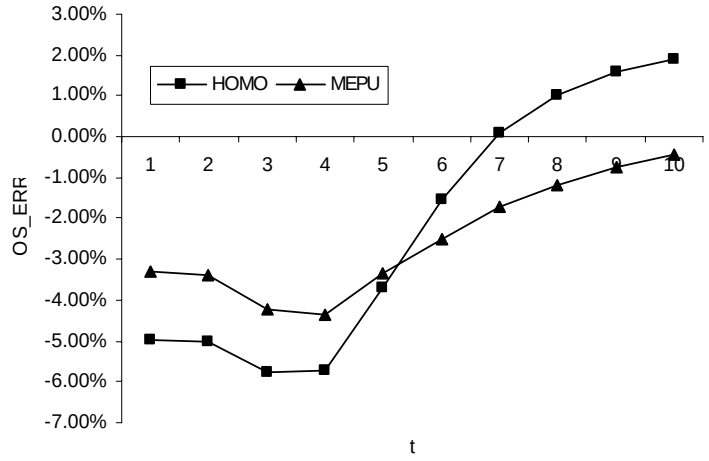

Figure 10: The relative error of the overall stress $\bar{\sigma}_{22}$ vs. load increment

Acknowledgment

The financial supports of National Science Foundation under grants CMS- 0310596, 0303902, 0408359 and Sandia contract DE-ACD4-94AL85000, ONR contract N00014-97-1-0687 are gratefully acknowledged.

Appendix A: Nonlinear homogenization

There are two commonly used approaches aimed at generalizing linear mathematical homogenization theory to nonlinear problems. The first of these approaches is based on the instantaneous decomposition of the second term in the velocity field

$$\dot{u}_k^1 = \chi_{mnk}\left(\boldsymbol{y}\right)\dot{\varepsilon}_{mnx}^0\left(\boldsymbol{x}\right) \tag{24}$$

where $\chi_{mnk}(\boldsymbol{y})$ is an instantaneous influence function, which is recomputed at every macroscopic Gauss point, every iteration and every load increment within the global Newton method. This approach has been successfully used in the context of rate-dependent, rate-independent plasticity and damage mechanics models and for problems involving small and large deformation (sees for instance [35]). It is very convenient for deriving a nonlinear variant of MEPU because by calculating $\chi_{mnk}(\boldsymbol{y})$ instantaneous enriched shape functions are directly obtained as described in detail below.

For completeness, it is instructive to mention an alternative nonlinear homogenization approach, which does not use the instantaneous decomposition (24). Instead, a nonlinear unit cell problem is stated as

$$\sigma^0_{ij,y_j}(\mathbf{y},t) \equiv f\left(\boldsymbol{\varepsilon}^{(n)}, \Delta\boldsymbol{\varepsilon}^0, \Delta\boldsymbol{\varepsilon}^1\right) = 0$$

where $\Delta\boldsymbol{\varepsilon}^0$ is (known) macroscopic strain gradient computed at every Gauss point in the macro-problem and $\Delta\boldsymbol{\varepsilon}^1$ is unknown microscopic strain field found by solving the nonlinear unit cell problem. The unit cell problem can be solved using weighted residual method, which states:

$$\begin{aligned}
&\textit{Find} \quad \Delta u^1 \textit{ such that}: \\
&r \equiv \int_\Theta \mathbf{B}^T \boldsymbol{\sigma}^0\left(\boldsymbol{\varepsilon}^{(n)}, \Delta\boldsymbol{\varepsilon}^0, \Delta\boldsymbol{\varepsilon}^1\right) d\Theta = 0 \quad \textit{on} \quad \Theta \\
&\textit{subjected to periodic} \quad \Delta u^1 \quad \textit{on} \quad \partial\Theta
\end{aligned}$$

The two approaches provide similar results provided that the load increment is sufficiently small.

We now discuss in more detail the first approach, which is adopted in the present manuscript.

Consider governing equations (small deformation, nonlinear plasticity material model) given in Eq. (10). The asymptotic expansions for the displacements and velocities is given by

$$\begin{aligned}
u_i^\zeta(\boldsymbol{x}) &= u_i(\boldsymbol{x},\boldsymbol{y}) = u_i^0(\boldsymbol{x},\boldsymbol{y}) + \zeta u_i^1(\boldsymbol{x},\boldsymbol{y}) + \zeta^2 u_i^2(\boldsymbol{x},\boldsymbol{y}) + O\left(\zeta^3\right) \\
v_i^\zeta(\boldsymbol{x}) &= v_i(\boldsymbol{x},\boldsymbol{y}) = v_i^0(\boldsymbol{x},\boldsymbol{y}) + \zeta v_i^1(\boldsymbol{x},\boldsymbol{y}) + \zeta^2 v_i^2(\boldsymbol{x},\boldsymbol{y}) + O\left(\zeta^3\right)
\end{aligned}$$

where $v_i^\zeta = \dot{u}_i^\zeta$. The chain rule for the differentiation is given by: $f_{,x}^\zeta = f_{,x} + \zeta^{-1} f_{,y}$.

The strain tensor components are given by

$$\varepsilon_{ij}^\zeta = \zeta^{-1}\varepsilon_{ij}^{-1} + \zeta^0\varepsilon_{ij}^0 + \zeta^1\varepsilon_{ij}^1 + O\left(\zeta^2\right)$$

where

$$\varepsilon_{ijx}^k = u^k_{(i,x_j)}, \quad \varepsilon_{ijy}^k = u^k_{(i,y_j)}$$

and

$$\varepsilon_{ij}^{-1} = \varepsilon_{ijy}^{0}$$

$$\varepsilon_{ij}^{0} = \varepsilon_{ijx}^{0} + \varepsilon_{ijy}^{1}$$

$$\varepsilon_{ij}^{1} = \varepsilon_{ijx}^{1} + \varepsilon_{ijy}^{2}$$

Similarly, for small deformations the strain rate quantities are given as

$$\dot{\varepsilon}_{ij}^{\zeta} = \zeta^{-1}\dot{\varepsilon}_{ij}^{-1} + \zeta^{0}\dot{\varepsilon}_{ij}^{0} + \zeta^{1}\dot{\varepsilon}_{ij}^{1} + O\left(\zeta^{2}\right)$$

where

$$\dot{\varepsilon}_{ij}^{-1} = \dot{\varepsilon}_{ijy}^{0}$$

$$\dot{\varepsilon}_{ij}^{0} = \dot{\varepsilon}_{ijx}^{0} + \dot{\varepsilon}_{ijy}^{1}$$

$$\dot{\varepsilon}_{ij}^{1} = \dot{\varepsilon}_{ijx}^{1} + \dot{\varepsilon}_{ijy}^{2}$$

The expansion of the stress rates is given as

$$\dot{\sigma}_{ij}^{\zeta} = \zeta^{-1}\dot{\sigma}_{ij}^{-1} + \zeta^{0}\dot{\sigma}_{ij}^{0} + \zeta^{1}\dot{\sigma}_{ij}^{1} + O\left(\zeta^{2}\right)$$

where

$$\dot{\sigma}_{ij}^{k} = L_{ijkl}\dot{\varepsilon}_{kl}^{k}$$

The rate form of equilibrium equations is given as

$$\zeta^{-2}\dot{\sigma}_{ij,y_j}^{-1} + \zeta^{-1}\left(\dot{\sigma}_{ij,x_j}^{-1} + \dot{\sigma}_{ij,y_j}^{0}\right) + \zeta^{0}\left(\dot{\sigma}_{ij,x_j}^{0} + \dot{\sigma}_{ij,y_j}^{1} + \dot{b}_i\right) + O\left(\zeta\right) = 0$$

from where the $O\left(\zeta^{-2}\right)$ rate equilibrium equation yields

$$\dot{\sigma}_{ij,y_j}^{-1} = \left(L_{ijkl}\dot{\varepsilon}_{kly}^{0}\right)_{,y_j} = 0$$

Pre-multiplying above by $\dot{u}_i^0$ and taking the integral over the unit cell domain yields

$$\int_{\Theta}\dot{u}_i^0\left(L_{ijkl}\dot{\varepsilon}_{kly}^{0}\right)_{,y_j}d\Theta = -\int_{\Theta}\dot{u}_{(i,y_j)}^{0}L_{ijkl}\dot{u}_{(k,y_l)}^{0}d\Theta + \underbrace{\int_{\partial\Theta}\dot{u}_i^0\dot{\sigma}_{ij}^{-1}n_j d\Gamma}_{=0 \text{ by periodicity}}$$

Assuming that the instantaneous properties remain positive definite yields

$$\dot{u}_{k,y_l}^{0} = 0 \quad or \quad \dot{u}_i^0 = \dot{u}_i^0\left(\boldsymbol{x}\right)$$

The $O\left(\zeta^{-1}\right)$ rate equilibrium equation is

$$\dot{\sigma}_{ij,x_j}^{-1} + \dot{\sigma}_{ij,y_j}^{0} = 0$$

Since $\dot{u}_i^0 = \dot{u}_i^0\left(\boldsymbol{x}\right) \Rightarrow \dot{\varepsilon}_{kly}^{0} = 0 \Rightarrow \dot{\sigma}_{ij}^{-1} = 0$, it follows that

$$\left[L_{ijkl}\left(\dot{\varepsilon}_{klx}^{0} + \dot{\varepsilon}_{kly}^{1}\right)\right]_{,y_j} = 0$$

Consider the separation of variables in the form of

$$\dot{u}_k^1 = \chi_{mnk}\left(\boldsymbol{y}\right)\dot{\varepsilon}_{mnx}^{0}\left(\boldsymbol{x}\right)$$

$$\dot{\varepsilon}_{kly}^{1} = \dot{u}_{(k,y_l)}^{1} = \dot{\varepsilon}_{mnx}^{0}\chi_{mn(k,y_l)} = \dot{\varepsilon}_{mnx}^{0}\phi_{mnkl}$$

which yields:

$$\left[L_{ijkl}\left(\dot{\varepsilon}_{klx}^{0} + \dot{\varepsilon}_{mnx}^{0}\phi_{mnkl}\right)\right]_{,y_j} = 0$$

or

$$\dot{\varepsilon}^0_{mnx}\left[L_{ijkl}\left(I_{klmn}+\phi_{mnkl}\right)\right]_{,y_j}=0 \quad \forall \dot{\varepsilon}^0_{mnx}$$

The resulting instantaneous unit cell problem is given by

$$\left[L_{ijkl}\left(I_{klmn}+\phi_{mnkl}\right)\right]_{,y_j}=0$$

The $O(1)$ equilibrium equation is given by

$$\sigma^0_{ij,x_j}+\sigma^1_{ij,y_j}+b_i=0$$

Taking the integral over the unit cell domain and exploiting periodicity yields

$$\frac{1}{|\Theta|}\int_\Theta \sigma^0_{ij,x_j}d\Theta+\frac{1}{|\Theta|}\int_\Theta b_i d\Theta=0$$

or

$$\left[\bar{\sigma}_{ij}\right]_{,x_j}+\bar{b}_i=0$$

5. References

1 J. Fish, and Z. Yuan, "Multiscale enrichment based on partition of unity". *International Journal for Numerical Methods in Engineering* 2005; **62**:1341-1359.

2 C.D. Mote, "Global-Local Finite Element Method," *International Journal for Numerical Methods in Engineering*, Vol. 3, pp. 565-574, 1971.

3 J. Fish, "The s-version of the finite element method," *Computers and Structures*, Vol. 43, No. 3, pp. 539-547, 1992.

4 J. Fish and S.Markolefas, "Adaptive s-method for linear elastostatics," *Computer Methods in Applied Mechanics and Engineering*, Vol. 103, pp. 363-396, 1993.

5 J. Fish and S.Markolefas, R.Guttal and P.Nayak, "On adaptive multilevel superposition of finite element meshes," *Applied Numerical Mathematics*, Vol 14., pp. 135-164, 1994.

6 J.W. Park, J.W. Hwang and Y.H. Kim, "Efficient finite element analysis using mesh superposition technique," *Finite elements in analysis and design*, Vol. 39, pp. 619-638, 2003.

7 J. Fish, "Hierarchical modeling of discontinuous fields," *Communications in Applied Numerical Methods*, Vol. 8, pp. 443-453, 1992.

8 J. Fish, N.Fares and A.Nath, "Micromechanical elastic cracktip stresses in a fibrous composite," *International Journal of Fracture*, Vol. 60, pp. 135-146, 1993.

9 J. Fish and A. Wagiman, "Multiscale finite element method for heterogeneous medium," *Computational Mechanics: The International Journal*, Vol. 12, pp. 1-17, 1993.

10 J.Fish and S.Markolefas, "The s-version of the finite element method for multilayer laminates," *International Journal for Numerical Methods in Engineering*, Vol. 33, no. 5, pp. 1081-1105, 1992.

11 D.H. Robbins and J.N. Reddy, "Variable kenematic modeling of laminated composite plates," *International Journal for Numerical Methods in Engineering*, Vol. 39, pp. 2283-2317, 1996.

12 N. Takano, M. Zako, and M. Ishizono, "Multi-scale computational method for elastic bodies with global and local heterogeneity," *J. Computer-Aided Material Design*, Vol. 7, pp. 111-132, 2000.

13 J. Fish and V.Belsky, "Multigrid method for a periodic heterogeneous medium. Part I: Convergence studies for one-dimensional case," Comp. Meth. Appl. Mech. Engng., Vol. 126, pp. 1-16, (1995).

14 J. Fish and V. Belsky, "Multigrid method for a periodic heterogeneous medium. Part 2: Multiscale modeling and quality control in mutidimensional case," *Computer Methods in Applied Mechanics and Engineering*, Vol. 126, 17-38, 1995.

15 J.Fish, A.Suvorov and V.Belsky,'Hierarchical Composite Grid Method for Global-Local Analysis of Laminated Composite Shells,' *Applied Numerical Mathematics*, Vol. 23, pp.241-258, (1997).

16 J. Fish and W. Chen, "Discrete-to-Continuum Bridging Based on Multigrid Principles," *Computer Methods in Applied Mechanics and Engineering*, Vol. 193, pp. 1693-1711, 2004.

17 T. Belytschko and T. Black, "Elastic crack growth in finite elements with minimal remeshing," *International Journal for Numerical Methods in Engineering*, Vol. 45, No. 5, pp. 601-620, 1999.
18 N. Moës, J. Dolbow and T. Belytschko, A finite element method for crack growth without remeshing, *International Journal for Numerical Methods in Engineering*, Vol. 46, No. 5, pp. 131-150, 1999.
19 T. Belytschko, N. Moës, S. Usui, C. Parimi, "Arbitrary discontinuities in finite element," *International Journal for Numerical Methods in Engineering*, Vol. 50, pp. 993-1013, 2001.
20 T. Strouboulis, I. Babuska and K. Copps, "The generalized finite element method: An example of its implementation and illustration of its performance," *International Journal for Numerical Methods in Engineering*, Vol. 47, pp. 1401-1417, 2000.
21 T. Strouboulis, I. Babuska and K. Copps, "The generalized finite element method," *Computer Methods in Applied Mechanics and Engineering*, Vol. 190, pp. 4081-4193, 2001.
22 J. T. Oden, I. Babuska, C.E. Baumann, "A discontinuous hp finite element method for diffusion problems," Journal of Computational Physics, Vol. 146, pp. 1-29, 1998.
23 S. S. Collis and Y. Chang, "The DG/VMS method for unified turbulence simulation," AIAA paper 2002-3124, 2002.
24 J. Chessa, H.W. Wang and T. Belytschko, "On the construction of blending elements for local partition of unity enriched finite elements," *International Journal for Numerical Methods in Engineering*, Vol. 57, No. 7, pp. 1015-1038, 2003.
25 I. Babuska, G. Caloz and J. E. Osborn, "Special finite element methods for a class of second order elliptic problems with rough coefficients," *SIAM. J. Numer. Anal.*, Vol. 4, pp. 945-981, 1994.
26 I. Babuska and J.M. Melenk, "The partition of unity finite element method: Basic theory and applications," *Computer Methods in Applied Mechanics and Engineering*, Vol. 139, pp. 289-314, 1996.
27 T. Belytschko and T. Black, "Elastic crack growth in finite elements with minimal remeshing," *International Journal for Numerical Methods in Engineering*, Vol. 45, No. 5, pp. 601-620, 1999.
28 G. J. Wagner, N. Moes, W.K. Liu, and T. Belytschko, "The Extended Finite Element Method for Rigid Particles in Stokes Flow," *International Journal for Numerical Methods in Engineering*, Vol. 51, pp. 293-310, 2001.
29 T. Strouboulis, I. Babuska and K. Copps, "The generalized finite element method: An example of its implementation and illustration of its performance," *International Journal for Numerical Methods in Engineering*, Vol. 47, pp. 1401-1417, 2000.
30 T. Strouboulis, I. Babuska and K. Copps, "The generalized finite element method," *Computer Methods in Applied Mechanics and Engineering*, Vol. 190, pp. 4081-4193, 2001.
31 J. Fish, P.Nayak, and M.H.Holmes, "Microscale Reduction Error Indicators and Estimators for a Periodic Heterogeneous Medium," *Computational Mechanics: The International Journal*, Vol. 14, pp. 1-16, 1994.
32 W. Chen and J. Fish, "A Generalized Space-Time Mathematical Homogenization Theory for Bridging Atomistic and Continuum Scales," submitted to International Journal for Numerical Methods in Engineering (2005)
33 E. F. Rybicki and M. F. Kanninen, "A Finite Element Calculation of Stress Intensity Factors by a Modified Crack Closure Integral," *Engineering Fracture Mechanics*, Vol. 9, pp. 931-938, 1977.
34 I. Babuska and J. E. Osborn. Generalized finite element methods: their performance and their relation to mixed methods. SIAM. J. Numer. Anal., Vol. 20, pp. 510-536, (1983).
35 J. Fish and K. L. Shek, "Finite Deformation Plasticity of Composite Structures: Computational Models and Adaptive Strategies," Comp. Meth. Appl. Mech. Engng., Vol. 172, pp. 145-174, (1999).
36 J. C. Simo and T. J. R. Hughes, "Computational Inelasticity," (Springer-Verlag, 1998).